Cavendish-HEP-96/15
DFTT 49/96
November 1996

$e^+e^- \to H^+H^-$ signals at LEP2 energies in the Minimal Supersymmetric Standard Model

Stefano Moretti[a,b] and Kosuke Odagiri[a]

a) Cavendish Laboratory, University of Cambridge,
Madingley Road, Cambridge CB3 0HE, UK.

b) Dipartimento di Fisica Teorica, Università di Torino,
and I.N.F.N., Sezione di Torino,
Via Pietro Giuria 1, 10125 Torino, Italy.

Abstract

In this paper we compare H^+H^- and W^+W^- into four-fermion production at centre-of-mass energies typical of LEP2 and somewhat larger. The theoretical framework considered is the Minimal Supersymmetric Standard Model. The interest in exploiting the e^+e^- CERN collider at values of $\sqrt{s}$ greater than 192 GeV could come from the discovery of Supersymmetric signals during runs at lower energy. If these indicate that a charged Higgs boson exists in the mass range $M_H \approx 95 - 105$ GeV, then a few years of running at $\sqrt{s} = 205 - 215$ GeV and nominal luminosity could make the detection of such scalars feasible, in the purely leptonic channel $\tau\nu_\tau\tau\nu_\tau$ and, for small $\tan\beta$'s, also in the semi-hadronic(leptonic) one jj$\tau\nu_\tau$. Charged Higgs bosons of the above nature cannot be produced by the beam energies approved at present for LEP2. However, if runs beyond the so-called '192 GeV cryogenic limit' will be approved by the CERN Council, our selection procedure will enable us to establish the presence, or otherwise, of charged Higgs bosons in the mentioned mass range.

Electronic mails: moretti,odagiri@hep.phy.cam.ac.uk

1. Introduction

The LEP2 collider [1] has already started operations. Event samples have been collected so far at $\sqrt{s} \approx 130$ and 161 GeV as well as at $\sqrt{s} \approx 172$ GeV. Further runs are scheduled at 192 GeV. Although not yet approved, the value $\sqrt{s} = 205$ GeV has also been considered in the context of the 1995 LEP2 Workshop [1]. From the results reported so far by the LEP Collaborations, it can be inferred that at present, contrary to the first excitement (which led many to believe in the evidence of some physics in the Supersymmetric sector), the data from the runs above the Z peak are in fair agreement with the Standard Model ($\mathcal{SM}$) expectations [2][1].

However, it is one of the primary goals of the LEP2 CERN collider to possibly bring some new insight to clarify whether already at its energy scale physics beyond the $\mathcal{SM}$ exists or not, particularly in the Higgs sector of the electroweak (EW) interactions [4]. In this respect, one of the most appealing theoretical framework is the Minimal Supersymmetric Standard Model ($\mathcal{MSSM}$). In fact, being a Supersymmetric (SUSY) theory, it provides a solution to the hierarchy problem via the cancellations of the infinities arising in the $\mathcal{SM}$ when computing quartic corrections to the Higgs mass and, at the same time, these can be kept under control if SUSY breaking occurs sufficiently near the electroweak scale $G_F^{-1/2}$. Moreover, if it does so and if it is combined with Grand Unification Theories, the $\mathcal{MSSM}$ predicts a value for the Weinberg angle θ_W in good agreement with the measured one and a value for the Grand Unification Mass that can explain the non-observed proton decay [5]. It also supplies a natural candidate for the dark matter in terms of the Lightest Supersymmetric Particle ($\mathcal{LSP}$), which is stable, neutral and weakly interacting (the neutralino).

The structure of the Higgs sector of the $\mathcal{MSSM}$ is determined at tree-level by only two parameters[2]: for example, M_A (the mass of the pseudoscalar Higgs) and $\tan\beta$ (the ratio between the vacuum expectation values associated with the two Higgs doublets, one giving masses to the up-type and the other to the down-type fermions). Thus, such a model is also rather predictive, not much less than the $\mathcal{SM}$, for which one parameter (the Higgs mass M_ϕ) is needed to describe its phenomenology. Other than the pseudoscalar neutral Higgs A, the $\mathcal{MSSM}$ Higgs spectrum involves other four scalars: the $\mathcal{CP}$–even neutral H and h, and the two charged $H^\pm$'s.

The search for Higgs bosons of the $\mathcal{MSSM}$ at LEP2 will be based mainly on the Higgs-strahlung process $e^+e^- \to Zh$ and on the associated production $e^+e^- \to Ah$ [6]. These

[1]Although it should be mentioned that the ALEPH Collaboration still claims to see in its data a rather significant excess of four-jet events in the sum of the di-jet masses at ≈ 105 GeV, at all LEP2 energies considered so far [3]. In contrast, the other Collaborations have never established the presence of similar effects.

[2]At one-loop also the top mass and the squark masses are needed. For these, we assume throughout the paper: $m_t = 175$ GeV and $M_S = 1$ TeV.

two mechanisms are somehow complementary. In fact, for small values of $\tan\beta$ the first process dominates, whereas at large $\tan\beta$'s the second reaction becomes quantitatively more important [4] (provided it is kinematically allowed). Typical cross sections are of the order of one picobarn or so. The dominant decay modes of both the h and A scalars are into $b\bar{b}$ and $\tau^+\tau^-$ pairs[3] [9]. Concerning the heavy neutral Higgs H, it should be noted that its mass (being much larger than the Z mass) implies that the chances for H production are confined to a tiny corner of the $(M_A, \tan\beta)$ parameter space (i.e., very small M_A and $\tan\beta$), where the cross section is very small and also P-wave suppressed at threshold [4].

The situation for the charged Higgs $H^\pm$ is apparently even less optimistic and extremely complicated. Indeed, the cross section for charged Higgs boson production via the channel $e^+e^- \rightarrow H^+H^-$ [8, 10] (although not particularly small at LEP2) yields a signal which is very hard to extract, because of the huge irreducible background in $e^+e^- \rightarrow W^+W^-$ events. In fact, on the one hand, the $\mathcal{MSSM}$ mass relations tell us (at tree-level) that ${M_{H^\pm}}^2 = {M_{W^\pm}}^2 + {M_A}^2$ and, on the other hand, kinematic bounds dictated by the LEP2 centre-of-mass (CM) energy imply that only $H^\pm$ scalars with mass $M_{H^\pm} \lesssim \sqrt{s}/2$ can be produced. Since the highest CM energy run scheduled for the CERN machine is at $\sqrt{s} = 192$ GeV, this realistically means that only charged Higgses with $M_{H^\pm} \lesssim 90$ GeV can have a sizable cross section at LEP2. Having at present the lower limit on the $\mathcal{MSSM}$ charged Higgs mass set at 85 GeV, this leaves only a small window at LEP2. Furthermore, in the above region, the $H^\pm$ and $W^\pm$ bosons are almost degenerate in mass, such that the differential distributions involving their decay products can hardly be useful in disentangling the two signals, especially considering that at $\sqrt{s} \approx 200$ GeV the cross section for W^+W^- production is almost three orders of magnitude larger than that for H^+H^-[4] ! The typical signature of a $H^\pm$ scalar would be most likely an excess of τ events with respect to the rates predicted by the $\mathcal{SM}$ (*lepton universality breaking* signal), as the lepton-neutrino decay channel has the largest branching ratio (BR). For small $\tan\beta$'s, hadronic channels can be also considered [4], together with the analysis of 'cascade' decays $H^\pm \rightarrow W^{\pm *}h, W^{\pm *}A$ (with $h, A \rightarrow b\bar{b}$).

It is the purpose of this study to reanalyse the discovery potential of $H^\pm$ particles of the $\mathcal{MSSM}$ at the LEP2 machine at CM energies of not only 205 GeV but also higher, for example: $\sqrt{s} = 210$ and 215 GeV. We stress that increasing $\sqrt{s}$ would generally bring some advantages in the above respect, and that a 10 GeV difference in $\sqrt{s}$ could be crucial to detecting charged Higgses of masses up to 100 GeV or so.

---

[3]In certain areas of the Supersymmetric parameter space Higgs particles can also decay into the SUSY-partners of ordinary particles, such as into invisible $\chi_1^0\chi_1^0$ ($\mathcal{LSP}$) pairs or via other modes involving charginos and/or neutralinos [7, 8].

[4]Note that the mentioned mass relation does not hold in non-minimal (NM) SUSY extensions of the $\mathcal{SM}$, for which the only lower mass constraint comes from LEP1 data, $M_{H^\pm}^{\rm NM} \gtrsim 44$ GeV [4]. In this context, LEP2 has a good potential for the charged Higgs boson discovery, especially for $M_{H^\pm} < M_{W^\pm}$ [4].

- First, the window in $M_{H^\pm}$ that could be explored would be larger.
- Second, if a $H^\pm$ scalar with a mass significantly larger than that of the $W^\pm$ (say, by 20 GeV) can be produced, then the different kinematics of their decay products (jet and leptons) can be fully exploited. In practise, particles arising from the $H^\pm$'s would have in the collider CM the same kinematics as in the decay frames of the scalars, whereas those coming from the $W^\pm$'s would have a significant boost.
- Third, even compared to the rates at 205 GeV, increasing $\sqrt{s}$ up to 215 GeV would enhance the cross section of H^+H^- production by a factor of four (for $M_{H^\pm} \approx 100$ GeV), whereas that for the creation of W^+W^- pairs would remain roughly constant.

The motivations for considering a run at a CM energy larger than the highest one scheduled at present for LEP2, in view of a possible $H^\pm$ detection, could be justified by two scenarios that could well occur at previous energy stages.

1. One or more Higgs bosons are discovered and these match the $\mathcal{MSSM}$ particle spectrum (i.e., a h or/and an A scalar). In addition, the corresponding masses are so light that they are consistent with a value of $M_{H^\pm}$ just beyond the reach of $\sqrt{s} = 192$ GeV. For example, note that, for $M_A \approx 60$ GeV, the $\mathcal{MSSM}$ predicts $M_h \approx 55 - 60$ GeV and $M_{H^\pm} \approx 100$ GeV, but the corresponding H^+H^- cross section is too small even at 205 GeV [4].
2. Some other $\mathcal{MSSM}$ signal is detected, and this is compatible with a charged Higgs boson around 100 GeV. For example, for h and A masses below 70 GeV (corresponding to $M_{H^\pm} \lesssim 106$ GeV) and for relatively small $\tan\beta$, there are still $(M_A, \tan\beta)$ open windows for $h, A \rightarrow$ neutralinos decays [8, 11].

If one of these two cases occurs, then it might be conceivable to put some more effort to increasing the discovery potential of a machine already existing, rather than to wait more years until the same Higgs mass domain can be covered by other machines (in particular, the LHC and the NLC).

The possibility of running the LEP2 machine at CM energies of 205 GeV or more has been already studied in the context of the LEP2 Workshop [12] (see also Ref. [13]), even though the maximum CM energy stage approved to date by the CERN Council is 192 GeV. (In particular, Ref. [12] considered beam energies up to 104 GeV.) Indeed, a beam energy of 96 GeV (Phase IV) represents a clear 'turning point' in the 'LEP Energy Upgrade Programme', as beam energies larger than that would require an upgrade of the cryoplants (Phases X and Y) now in use at LEP, because of their limited cooling power. In this respect, however, we would like to stress that the three values $\sqrt{s} = 205, 210$ and 215 GeV are *all* beyond the present so-called 'cryogenic limit', such that they would require the same kind of layout modifications and equipment fittings. Furthermore, we remind the reader the following statement in the LEP2 Proceedings (incidentally, precisely where the $\mathcal{SM}$ and the $\mathcal{MSSM}$ Higgs sectors are compared to each other): "*It could however be imagined that if a new particle were discovered, a substantial extension of the LEP2 project could be decided upon with the purpose of identifying this particle*" [14]. We push our attitude even further, by saying that if this particle is a $\mathcal{MSSM}$ one and this tell us that some more $\mathcal{MSSM}$ physics is just *beyond the corner*, such an *extension* could also well be in the direction of a further beam energy upgrade. In contrast, if none of the above options (i.e., 1. and 2.) is verified, the prospect of LEP2 running at 205 GeV or above that would have no special meaning from our viewpoint.

The plan of the paper is as follows. In Section 2 we describe our computational technique and give the values of the parameters used. In Section 3 we present and discuss our results. In Section 4 we draw our conclusions.

2. Calculation

Many analytical formulae exist to compute the total cross section for on-shell H^+H^- production [10, 15]. In contrast, the literature on the off-shell production, followed by the decays of the two bosons (for example, into four fermions) is more limited. Thus, in carrying out our analysis we have decided to recompute the matrix element for the $2 \to 4$ process

$$e^+e^- \to H^+H^- \to f_1\bar{f}_2f_3\bar{f}_4, \tag{1}$$

where $f_{1,2,3,4}$ represent generic fermions. To this end we have proceeded in the following way. First, we have used the helicity amplitude techniques described in Refs. [16, 17, 18] to produce a `FORTRAN` code computing the Feynman amplitude squared of process (1). Furthermore, this has been counter-checked against a second program built up by using the subroutines contained in the package `HELAS` [19], which indeed include scalar-fermion vertices (for the Goldstone bosons of the $\mathcal{SM}$), with the couplings rearranged to the values predicted by the $\mathcal{MSSM}$. Finally, a third program implementing formulae obtained by using the textbook method of tracing the γ-matrices was also generated. The results obtained with the three different formalisms agree within twelve figures in `REAL*8` precision. The matrix elements have been then integrated over the phase space and the distributions produced by resorting to a multidimensional integration making use of the Monte Carlo (MC) routine `VEGAS` [20]. Also to compute the rates for the $\mathcal{SM}$ reaction

$$e^+e^- \to W^+W^- \to f_1\bar{f}_2f_3\bar{f}_4 \tag{2}$$

we have proceeded as above. We are aware that a huge number of analytical, semi-analytical and numerical calculations are available in literature for reaction (2) [21]. However, to our purposes, it was more useful to have a handy program, constructed on the same footing as that for four-fermion production via H^+H^-, with the advantage of offering a straightforward comparison between the rates of the two mechanisms (1)–(2).

Concerning the possible signatures of process (1) and (2), one can expect

$$H^+H^-, W^+W^- \rightarrow \mathrm{jjjj}, \qquad \text{hadronic channel,} \tag{3}$$

$$H^+H^-, W^+W^- \rightarrow \mathrm{jj}\tau\nu_\tau, \qquad \text{semi} - \text{hadronic(leptonic) channel,} \tag{4}$$

$$H^+H^-, W^+W^- \rightarrow \tau\nu_\tau\tau\nu_\tau, \qquad \text{leptonic channel.} \tag{5}$$

In the following, we will consider all of them.

A few details now, concerning the numerical values of the parameters entering in the calculation. The numbers adopted are: $\alpha_{em} = 1/128$, $\sin^2\theta_W = 0.2320$, $M_Z = 91.1$ GeV, $\Gamma_Z = 2.5$ GeV, $M_{W^\pm} \equiv M_Z\cos\theta_W \approx 80$ GeV and $\Gamma_{W^\pm} = 2.2$ GeV, while for the fermion masses we have used $m_\tau = 1.78$ GeV, $m_{\nu_\tau} = m_u = m_d = 0$, $m_s = 0.3$ GeV and $m_c = 1.4$ GeV. The $H^\pm$ mass has been computed using the tree-level relation $M^2_{H^\pm} = M^2_A + M^2_{W^\pm}$, as one-loop corrections are small [22]. The $H^\pm$ width has been taken from Ref. [9]. The strong coupling constant α_s, which enters in the *running masses* of the quarks (for details, see Ref. [9]) when calculating $H^\pm \rightarrow cs$ decays, has been evaluated at the two loop order, with $\Lambda^{(4)}_{\overline{\mathrm{MS}}} = 230$ MeV, at the scale $Q^2 = s$.

To allow for large rates in the hadronic and semi-hadronic(leptonic) Higgs decay channels, we have restricted our attention to the case of small values of $\tan\beta$, since for large values the $H \rightarrow cs$ channel becomes negligible. For reference, in presenting our results we will adopt the choice $\tan\beta = 1.5$[5]. Finally, for the mass of the charged Higgs boson we will use the value $M_{H^\pm} \approx 100$ GeV (that is, $M_A = 60$ GeV). However, we will generalise in the end our conclusions also to other values of the two $\mathcal{MSSM}$ parameters.

A brief comment is in order before ending this section, concerning higher order corrections to processes (1)–(2). Many of these are well known in literature, in both cases [23, 24]. However, we have not included them in our analysis. In fact, on the one hand, we are interested in establishing effects (differences in total and differential rates between the two processes) whose relative magnitude must be well beyond the effects due to radiative corrections, in order to be detectable. On the other hand, higher order results can be easily incorporated (in the case of process (1)) or are already included (in the case of process (2)) in many of the calculations available in literature. In the very end, in fact, our results should be reproduced by the various event generators [25] that are in possess of the four LEP2 Collaborations and which include all the above corrections, together with a simulation of the various detector and hadronisation effects, which are clearly beyond our capabilities.

[5]Note that the $\tan\beta$ dependence of process (1) enters when considering Higgs decays, since the rates of the on-shell production depend only on $M_{H^\pm}$.

3. Results

For the values that we have assumed for $\tan\beta$, $M_{H^\pm}$ and $M_{W^\pm}$, the total cross sections for processes (1)–(2) are displayed in the upper sections of Tab. Ia, b and c (in correspondence to the three mentioned decay channels). The values of energies considered are $\sqrt{s} = 205, 210$ and 215 GeV. From those numbers it is clear that, if no appropriate Higgs selection procedure is exploited, the chances of disentangling H^+H^- signals from the enormous W^+W^- backgrounds are practically nil: and this is true for all decay channels (3)–(5) and CM energies as well. Differences are dramatic in the four-jet channel, but these gradually diminish if the lepton-neutrino decays are selected. Nevertheless, at this stage, the H^+H^- rates are at the most 12% of the W^+W^- ones (this occurs at $\sqrt{s} = 215$ GeV for the leptonic signature). This is too little, further considering that in the $\tau\nu_\tau\tau\nu_\tau$ channel invariant mass spectra for the decay products of the two bosons cannot be reconstructed because of the presence of *two neutrinos*.

The relative statistical importance of the rates in Tab. I for the three channels (3)–(5) can be understood in term of the corresponding branching ratios (BRs) (see, e.g., Ref. [9])[6]:

$$BR(H^+H^- \to \mathrm{jjjj}) \approx 1\%, \qquad BR(W^+W^- \to \mathrm{jjjj}) \approx 50\%, \tag{6}$$

$$BR(H^+H^- \to \mathrm{jj}\tau\nu_\tau) \approx 20\%, \qquad BR(W^+W^- \to \mathrm{jj}\tau\nu_\tau) \approx 14\%, \tag{7}$$

$$BR(H^+H^- \to \tau\nu_\tau\tau\nu_\tau) \approx 63\%, \qquad BR(W^+W^- \to \tau\nu_\tau\tau\nu_\tau) \approx 1\%. \tag{8}$$

In general, it has to be said that leptonic decays favour $H^\pm$ signals, whereas hadronic decays favour $W^\pm$ backgrounds, this behaviour being dictated by the interplay between the values of the fermion masses and $\tan\beta$ in the scalar-fermion-fermion couplings. In fact, one gets that $BR(H^\pm \to \tau\nu_\tau)/BR(W^\pm \to \tau\nu_\tau) \approx 7$ and $BR(W^\pm \to \mathrm{jj})/BR(H^\pm \to \mathrm{jj}) \approx 6$.

As mentioned in the Introduction, there are systematical differences in the kinematics of events of the type (1)–(2) that could help in extracting the signals out of the backgrounds.

1. H^+H^- production proceeds via the s-channel only, whereas W^+W^- events can occur through t- and u-channels via the exchange of an electron neutrino. (i) As a consequence, in the latter case, one would expect to see in the spectrum of the angle of the $W^\pm$ boson(s) with respect to the beam a component peaking in the forward and/or backward direction. Indeed, it turns out that at LEP2 energies the contribution of the graph involving neutrino exchange is larger (by a factor of 2) than that of the graphs involving the triple gluon vertices γW^+W^- and ZW^+W^- (for details, see Ref. [26]). In contrast, in the former case, the angular distribution of the charged Higgs bosons should follow the $\sin^2\theta$ law typical of spin-zero particle production.

[6] Assuming again the mentioned values of $\tan\beta$ and $M_{H^\pm}$.

2. Since the $H^\pm$ bosons are produced via process (1) practically at rest, the kinematics of their decay products only depends on the actual value of $M_{H^\pm}$ and retains most of the features that it would have in the $H^\pm$ rest frame. In contrast, the $W^\pm$ decay products suffer from a boost, dictated by the value of the difference $\sqrt{s} - 2M_{W^\pm}$. Hence, one expects that, for example: (ii) the two fermions coming from the same $H^\pm$ decay are back-to-back in the collider CM frame; (iii) their transverse momentum has a low maximum value. These features are not shared by W^+W^- events.

We notice that only in one of the three cases (3)–(5) the above quantities can be defined unambiguously. This happens for the semi-hadronic(leptonic) channel. In the cases of the hadronic and leptonic signatures this is no longer true. In the former case, in only one of the three possible two-jet combinations the particles would come from the same decay. In the latter case, the presence of two neutrinos prevents one even from reconstructing the four-vectors of the particles that decay, as only three four-momenta can be assigned (one for each of the τ's and the one defined by using the missing energy and three-momentum). However, it is possible to remedy these two problems. Since the optimal solution depends on the signature considered, we treat separately the decays (3)–(5) in the three following subsections. Moreover, in the forthcoming Figs. 1–4, the cases (a), (b) and (c) will refer to the mentioned decays, in corresponding order, as in Tab. I[7].

3.1 The hadronic channel

In the case of the decays (3) there is an effective strategy to adopt, in order to assign the right pair of jets to the parent $H^\pm$: that is, to assume that the two quarks belonging to the same boson decay are those most far apart. In practise then, one can compute all the relative angles between the directions of the four jets and couple the two partons for which such an angle is largest. In contrast, the direction of any of the other two quarks from the other $H^\pm$ decay is distributed in a random way with respect to the previous two, such that only in a small corner of the phase space wrong assignments can occur. Naturally, what has just been said has also been done for W^+W^- events. In this case, however, wrong assignments will be more frequent, because the boosts on the decay products tend to shrink their relative angle.

Indeed, by looking at Fig. 1a, 2a and 3a, one realises that the correct assignment is made most of the times, as the variables plotted there largely retain the features that they would have if the tagging was straightforward[8]. In detail, the angle of the reconstructed boson (i.e., θ_B) follows to a large extent the expected $\sin^2\theta_\mathrm{B}$ (for H^+H^-) and $\cos^2\theta_\mathrm{B}$ (for W^+W^-)

[7]This has been done in order to facilitate the comparison among the various decay channels, at the cost of discussing the various figures in a different order respect to that in which they are plotted. Note also that distributions in Figs. 1–3 are normalised to unity, whereas those in Fig. 4 sum to the total cross sections.

[8]Compare to Figs. 1b, 2b and 3b for the semi-hadronic(leptonic) decays (see later on).

laws (Fig. 1a). At the same time, the relative angle of the two reconstructed jets (i.e., $\theta_{\rm ff}$) belonging to the same $H^\pm$ decay tends to be distributed at small cosines, whereas for those from the $W^\pm$ is much more spread out. Finally, the spectrum in transverse momentum of the two jets (i.e., p_T) is much softer in the former than in the latter case.

It is then clear from the figures that a Higgs selection strategy appears evident. For example, one can impose the following kinematic cuts: $|\cos\theta_{\rm B}| < 0.60$ (for all $\sqrt{s}$), plus $\cos\theta_{\rm ff} < -0.88(-0.80)[-0.72]$ and $p_{\rm T} < 24(34)[40]$ GeV, corresponding to $\sqrt{s} = 205(210)[215]$ GeV, to enhance the signal content in four-jet events. Unfortunately, this does not help much in the end. In fact, although the background contributions are cut out by a factor of $\approx 24(14)11$ at $\sqrt{s} = 205(210)[215]$ GeV, whereas the signal reduction is only ≈ 1.3 (at all energies), the cross sections of H^+H^- events are too small to be observable, around three orders of magnitude smaller than those for W^+W^- pairs (lower section of Tab. Ia). This can be seen in Fig. 4a, which shows the invariant mass spectrum of the two jets selected (i.e., $M_{\rm ff}$). The Higgs peaks are lost beneath the distributions of W^+W^- events, which (incidentally) hardly show a peak at 80 GeV.

3.2 The semi-hadronic(leptonic) channel

In the case of the semi-hadronic(leptonic) channel the assignment of the right pair of fermions to the parent boson is straightforward. Therefore, the differential spectra do not suffer from any distortion and reproduce exactly the features expected for the quantities plotted in Fig. 1b, 2b and 3b[9].

The Higgs selection procedure we adopt here is the same as was outlined in the previous section, as the behaviour of the various quantities are very similar in both cases. Contrary to hadronic decays, the final results in case of channel (4) are encouraging indeed. In fact, from Tab. Ib (lower part), one can notice that after the kinematic cuts, the rates of H^+H^- and W^+W^- events are now comparable, for all energies. Moreover, on the one hand, the selection procedure is here even more effective than in the hadronic channel and, on the other hand, the absolute numbers are much bigger than before. The cross section for W^+W^- has been reduced by a factor $\approx 1075(491)[336]$, whereas for H^+H^- events the numbers are again ≈ 1.3 (for all $\sqrt{s}$'s).

The invariant mass distributions of the two-jet pair (or equivalently, of the $\tau\nu_\tau$ pair, after the missing energy and three-momentum have been assigned to the neutrino) for case (4) are plotted in Fig. 4b. The bins there are 2 GeV wide. It is worth noticing that the curious shape of W^+W^- events is simply an effect of the cuts, with no special physics meaning. In fact, the mass spectra before the cuts have 'shoulders' (where the rates steeply drop) exactly

[9] Note that in Fig. 1b both the angle θ_+ and θ_- (that is of the W^+ and W^- respect to, say, the electron beam direction) are plotted, even though their distinction is possible in case of semi-hadronic(leptonic) decays.

where the 'spurious peaks' (those on the right in Fig. 4b) appear after the kinematic cuts. In fact, the latter strongly cut-off configurations around the $W^\pm$ mass, but not that much in regions further away. In the end (luckily enough), this leaves like a 'valley' precisely where the Higgs peaks clearly stick out, at all energies (and they would even if the actual mass resolution of the detectors will be much worse than 2 GeV: note the logarithmic scale in the figure).

3.3 The leptonic channel

The leptonic channel is probably the most complicated to select kinematically, because of the missing four-momentum due to the neutrinos. Nonetheless, the large decay rates of the Higgs scalars into $\tau\nu_\tau$ pairs furnish an appealing starting point. In this case it is no longer possible to reconstruct pairs of particles from the same boson decay in any way. The only thing which can reasonably be done is to define the various variables by using the only two four-momenta that can be tagged. Therefore, in this case: $\theta_{\rm B}$ is the angle of the system formed by the two τ's respect to the beam directions; $\theta_{\rm ff}$ is the angle between them; p_T their transverse momentum and $M_{\rm ff}$ their invariant mass.

No very distinctive features between the H^+H^- and W^+W^- decays appear in the spectrum of Fig. 1c, whereas some differences occur in Fig. 2c and 3c. The first plot somewhat resembles those of the channels (3)–(4), at least qualitatively. In fact, there is a sort of kinematic symmetry in the two decays of the bosons, with respect to each other, such that many of the phase space configurations occupied by a neutrino in one decay are also common to a lepton in the other one. Fig. 2c tells us that, in W^+W^- events, whichever is the orientation of the τ momenta, these tend to be aligned back-to-back by the boosts, as the two $W^\pm$'s fly apart after they are produced. In case of H^+H^- decays, where no boost acts, the distribution is flat. Furthermore, spin effects also act in the same direction. The shape of the curves in Fig. 3c follows from that in Fig. 1c. In particular, the tendency in W^+W^- samples of $|\cos\theta_{\rm B}|$ being closer to one implies that the corresponding p_T spectrum (proportional to $|\sin\theta_{\rm B}|$) is soft, whereas this does not occur for H^+H^-.

Having in mind the behaviours outlined in Fig. 1c, 2c and 3c, we have attempted, as Higgs selection procedure, the one defined by the following requirements on the phase space: $\cos\theta_{\rm ff} > -0.50$ and $p_{\rm T} > 50$ GeV, for $\sqrt{s} = 205, 210, 215$ GeV (the spectrum in $\cos\theta_{\rm B}$ is no longer useful). The rates that follow can be appreciated in Tab. Ic (lower part). Though much less than in the two previous cases, the signal-to-background ratio has been improved. In detail, the cross section for W^+W^- has been reduced by a factor $\approx 5.4(5.6)[6.0]$, whereas for H^+H^- events the numbers are $\approx 1.9(1.9)[1.9]$, corresponding to $\sqrt{s} = 205(210)[215]$ GeV.

Finally, the invariant mass spectra of the $\tau^+\tau^-$ pair is displayed in Fig. 4c. Since the energy of the leptons is more or less the same both in $H^\pm$ and $W^\pm$ decays (on average, 1/4 of the total CM energy) and since the τ's tend to be back-to-back in W^+W^- events (see Fig. 2c), their mass distributions are always shifted towards high values, whereas this is not the case for the H^+H^- sample (for which the $\cos\theta_{\rm ff}$ distribution is flat).

3.4 Non-resonant backgrounds

So far we have not mentioned that there are graphs that can produce the final states jjjj, jj$\tau\nu_\tau$ and $\tau\nu_\tau\tau\nu_\tau$ via e^+e^- annihilations without proceeding through H^+H^- and W^+W^- pair production and decay. These can be EW contributions (for all three final states) and QCD contributions as well (for the purely hadronic channel). In particular, the ZZ resonant EW diagrams (entering in the jjjj and $\tau\nu_\tau\tau\nu_\tau$ signatures) could well be large, as the CM energies considered here are above the ZZ threshold. In contrast, those involving γZ, $\gamma\gamma$ intermediate states (t and u channel graphs) as well as single resonant contributions (s channel graphs) are always much smaller. QCD diagrams can be large, though their kinematics is very different from that of the H^+H^- and W^+W^- resonant contributions. Indeed, we expect the kinematic selections adopted here to largely reduce the rates of background events.

We have calculated all these additional diagrams by using the [19] libraries, and counter-checked (where possible) their outputs against the well-known results given in literature [21], obtaining perfect agreement. After the signal selections adopted in this study and for the jj$\tau\nu_\tau$ and $\tau\nu_\tau\tau\nu_\tau$ channels, the differences are at the level of percent or less, so that, e.g., including the new diagrams and interfering them with processes (1) and (2) hardly modifies the distributions in Figs. 4a,b and c and the number in the low sections of Tabs. Ia–c. In particular, we notice that the larger effects (up to 7%, at $\sqrt{s} = 215$ GeV) occur in the leptonic channel. However, these are confined in the low invariant mass region of Fig. 4c, so that a further cut in that region (e.g., $M_{\rm ff} > 20$ GeV) allows one to remove completely the background events, without affecting dramatically the H^+H^- and W^+W^- rates. In case of the jjjj channel differences can be larger (especially depending on the selection criteria of the QCD events). However this is not relevant for our analysis as the purely hadronic channel is useless to our purposes (see Fig. 4a and Tab. Ia).

4. Conclusions

We conclude our paper in a rather optimistic way: in order to disentangle $H^\pm$ from $W^\pm$ decays (within the framework of the $\mathcal{MSSM}$), a higher energy option of LEP2 (beyond 200 GeV) could be helpful. In fact, on the one hand, it is certainly impossible to resort to hadronic decays but, on the other hand, semi-hadronic(leptonic) and leptonic decays would offer chances of detection. This is especially true at 215 GeV and for the jj$\tau\nu_\tau$ channel. In this case, after an appropriate kinematic selection, the integrated cross section of signal events is only approximately 23% smaller than that of background events. The number increases to $\approx 33\%$ at 210 GeV and to $\approx 40\%$ at 205 GeV. In this case, one can also rely on the invariant mass spectra (of the pair of fermions coming from the same boson decay) to disentangle $H^\pm$ peaks, which should be clearly visible on top of the $W^\pm$ background. For leptonic decays, the only way to assess the presence of charged Higgs signals is to look for lepton universality breaking in τ production. In this case, one gets an excess of events (with respect to the $\mathcal{SM}$ predictions) of the order of $\approx 8(21)[36]\%$, corresponding to the CM energies $\sqrt{s} = 205(210)[215]$ GeV. Furthermore, for the leptonic signature, some signal effects could also be visible in the distributions in the invariant mass of the detectable $\tau^+\tau^-$ pair.

We also stress that changing the value of $M_{H^\pm}$ (in the range in which Higgs signals are produced with large cross section, say between 95 and 105 GeV, for $\sqrt{s} = 215$ GeV) should not modify drastically the above conclusions. In contrast, the actual value of $\tan\beta$ is crucial, as the hadronic decay rates of the charged Higgs boson strongly depend on this parameter (the larger this is the smaller they are), especially because the semi-hadronic(leptonic) channel is the most promising one. In fact, for large values of $\tan\beta$ only the fully leptonic signature would be exploitable. In this case, however, the $H^+H^- \to \tau\nu_\tau\tau\nu_\tau$ rates would be larger than those presented here. For example, for $\tan\beta = 30$, the branching ratio of charged Higgses into $\tau\nu_\tau$-pairs is practically 100% (against 79% at $\tan\beta = 1.5$), so that the H^+H^- cross sections in Tab. Ic would be increased in the end by a factor ≈ 1.6, inducing an excess of $\tau\nu_\tau\tau\nu_\tau$ events of the order of $\approx 13(33)[58]\%$. Also note that the key features of our analysis are not exploitable for lighter $H^\pm$'s (those producible at 192 GeV and below), simply because their mass would be *degenerate* with that of the $W^\pm$ and most of the quantities we resorted to in the event selection would look identical in both the signal and the background. Furthermore, we add that the inclusion of the Initial State Radiation (ISR) should not modify the interplay between H^+H^- and W^+W^- events, as in general it would not affect their relative rates.

The crucial point seems to be in the end the number of H^+H^- events on which one can rely. In the two detectable channels, the typical signal cross sections are between 1 and 10 femtobarns (they are bigger at higher CM energies). Therefore, between 10 and 100 inverse picobarns would be needed at 215 GeV to produce one signal per year. Since this is roughly the luminosity which is expected to be collected at the various energy stages (per experiment), we expect that after a few years of running at the higher energy options considered here something like ten charged Higgs events of the $\mathcal{MSSM}$ could be detected. Finally, before closing we would like to make two final considerations.

Firstly, we remind the reader that we have carried out our analysis, which considers an increased LEP2 beam energy, under the assumption that this situation is conceivable only if the presence of SUSY signals was already established during runs at lower energies, with those indicating the existence of a charged Higgs $H^\pm$ with mass around 100 GeV (thus, beyond the reach of $\sqrt{s} = 192$ GeV). In other terms, one would be searching for something that he already knows is existing. Therefore, the *extension of the LEP2 project* that we have mentioned at the beginning could well be also finalised in accumulating as much luminosity as needed to assess the presence of the expected particle at the higher energies.

Secondly, we warn the reader that our results come from partonic calculations. No hadronisation or detector effects have been taken into account. Not even Initial State Radiation was implemented. Therefore before being taken as conclusive, these should be confirmed by the experimental simulations, by means of MC event generators, which include all the above aspects. Even because, in doing so, the Higgs selection procedures that we have adopted could also be improved, yielding more interesting arguments to the issue that we have raised here.

In the end, in the case that further upgrades beyond the '192 GeV limit' will be eventually considered by the CERN Council, we believe that our results should be kept into account when planning the activity of the machine at those new energy regimes.

Acknowledgements

We thank Ben Bullock for useful discussions. This work is supported in part by the Ministero dell' Università e della Ricerca Scientifica, the UK PPARC, and the EC Programme "Human Capital and Mobility", Network "Physics at High Energy Colliders", contract CHRX-CT93-0357, DG 12 COMA (SM). KO thanks Trinity College and the Committee of Vice-Chancellors and Principals of the Universities of the United Kingdom for financial support.

References

[1] Proceedings of the Workshop 'Physics at LEP2', eds. G. Altarelli, T. Sjöstrand and F. Zwirner, CERN Report 96-01.

[2] Aleph Collaboration, *preprint* CERN-PPE/96-10;
Delphi Collaboration, *preprint* CERN-PPE/96-75;
L3 Collaboration, *preprint* CERN-PPE/96-29;
Opal Collaboration, *preprint* CERN-PPE/96-20.

[3] See, for example:
F. Ragusa, talk presented at the meeting of the LEPC working group on 19 November 1996, CERN, Geneva.

[4] M. Carena and P.M. Zerwas (conveners), in Ref. [1], Section 'Higgs Physics' and references therein.

[5] See, for example:
G.G. Ross, in Proceedings of "*Joint International Lepton-Hadron Symphosium and Europhysics Conference on High Energy Physics*", Geneva, Switzerland, 25 July–1 August, 1992, eds. S. Hegarty *et al.*, Vol. I, and references therein.

[6] J.F. Gunion and H.E. Haber, *Nucl. Phys.* **B278** (1986) 449.

[7] J.F. Gunion and H.E. Haber, *Nucl. Phys.* **B307** (1988) 445.

[8] A. Djouadi, J. Kalinowski and P.M. Zerwas, *Z. Phys.* **C57** (1993) 569.

[9] S. Moretti and W.J. Stirling, *Phys. Lett.* **B347** (1995) 291; Erratum, *ibidem*, **B366** (1996) 451.

[10] S. Komamiya, *Phys. Rev.* **D38** (1988) 2158.

[11] A. Djouadi, P. Janot and J. Kalinowski, *Phys. Lett.* **B376** (1996) 220.

[12] S. Myers and C. Wyss, in Ref. [1], Section 'Physics/Machine Interface' and references therein.

[13] S. Myers and C. Wyss, 'LEP2 Energy Upgrade', LEP2 Note 95-34, August 1995;
ed. J. Poole, Proceedings of the Fifth Workshop on LEP Performance, CERN SL/95-08 (DI);
The Workshop on Physics at LEP2, 'Interim Report on the Physics Motivations for an Energy Upgrade of LEP2', *preprint* CERN-TH-95-151, CERN-PPE-95-78, CERN-PPE-95-078, C95-06-15.1, June 1995.

[14] In Ref. [4], page 423.

[15] See, for example:
Proceedings of the Workshop 'e^+e^- Collisions at 500 GeV. The Physics Potential', Munich, Annecy, Hamburg, 3–4 February 1991, ed. P.M. Zerwas, DESY pub. 92–123A/B/C, August 1992 and December 1993.

[16] R. Kleiss and W.J. Stirling, *Nucl. Phys.* **B262** (1985) 235.

[17] C. Mana and M. Martinez, *Nucl. Phys.* **B287** (1987) 601.

[18] S. Moretti, *Phys. Rev.* **D50** (1994) 2016.

[19] H. Murayama, I. Watanabe and K. Hagiwara, HELAS: HELicity Amplitude Subroutines for Feynman Diagram Evaluations, *KEK Report* 91-11, January 1992.

[20] G.P. Lepage, *Jour. Comp. Phys.* **27** (1978) 192.

[21] D. Bardin and T. Riemann, *Nucl. Phys.* **B462** (1996) 3;
E.E. Boos, M.N. Dubinin, V.F. Edneral, V.A. Ilin *et al.*, *Moscow State Univ. preprint* MGU-89-63/140 (1989); *preprint* KEK 92-47 (1992);
D. Bardin, M. Bilenky, D. Lehner, A. Olchevski and T. Riemann, in Proceedings of the Zeuthen Workshop on Elementary Particle Theory – Physics at LEP200 and Beyond, T. Riemann and J. Blümlein (eds.), Teupitz, Germany, April 10–15, 1994, *Nucl. Phys. (Proc. Suppl.)* **37B** (1994) 148;
D. Bardin, A. Leike and T. Riemann, *Phys. Lett.* **B353** (1995) 513;
F.A. Berends, R. Kleiss and R. Pittau, *Comp. Phys. Comm.* **85** (1995) 437; *Nucl. Phys.* **B424** (1994) 308; *Nucl. Phys.* **B426** (1994) 344; *Nucl. Phys. (Proc. Suppl.)* **37B** (1994) 163;
R. Pittau, *Phys. Lett.* **B335** (1994) 490;
F. Caravaglios and M. Moretti, *Phys. Lett.* **B358** (1995) 332;
C.G. Papadopoulos, *Phys. Lett.* **B352** (1995) 144;
D. Bardin, M. Bilenky, A. Olchevski and T. Riemann, *Phys. Lett.* **B308** (1993) 403; Erratum, hep-ph/9507277;
Minami-Tateya collaboration, KEK Report 92-19, 1993;
S. Kawabata, *Comp. Phys. Comm.* **88** (1995) 309;
M. Skrzypek, S. Jadach, W. Płaczek, and Z. Wąs, *Nucl. Phys.* **B449** (1995) 91;
T. Sjöstrand, *Comp. Phys. Comm.* **82** (1994) 74;
H. Anlauf, J. Biebel, A. Himmler, P. Manakos *et al.*, *Comp. Phys. Comm.* **79** (1994) 487;
G. Passarino, *preprint* February 1996, hep-ph/9602302;
E. Accomando and A. Ballestrero, *preprint* DFTT 16/96, July 1996;
G. Montagna, O. Nicrosini, G. Passarino and F. Piccinini, *Phys. Lett.* **B348** (1995) 178;
G. J. van Oldenborgh, P. J. Franzini, and A. Borrelli, *Comp. Phys. Comm.* **83** (1994) 14;
G. Montagna, O. Nicrosini and F. Piccinini, *Comp. Phys. Comm.* **90** (1995) 141.

[22] A. Brignole, J. Ellis, G. Ridolfi and F. Zwirner, *Phys. Lett.* **B271** (1991) 123;
A. Brignole, *Phys. Lett.* **B277** (1992) 313.

[23] A. Arhib and G. Moultaka, *preprint* PM/96-16, June 1996.

[24] See, for example:
W. Beenakker and F.A. Berends (conveners), in Ref. [1], Section 'WW Cross Sections and Distributions' and references therein.

[25] D. Bardin and R. Kleiss (conveners), in Ref. [1], Section 'Event Generators for WW physics' and references therein.

[26] G. Gounaris, J.-L. Kneur and D. Zeppenfeld (conveners), in Ref. [1], Section 'Triple Gauge Boson Couplings' and references therein.

Table Captions

[I] Cross section in femtobarns for processes (1)–(2), in the channels: (a) jjjj, (b) jj$\tau\nu_\tau$, (c) $\tau\nu_\tau\tau\nu_\tau$; for three different values of CM energy, before (upper section) and after (lower section) the following cuts: (a) and (b) $|\cos\theta_{\rm B}| < 0.60$ (for all $\sqrt{s}$), plus $\cos\theta_{\rm f\bar f}< -0.88(-0.80)[-0.72]$ and $p_{\rm T} < 24(34)[40]$ GeV, in correspondence of $\sqrt{s} = 205(210)[215]$ GeV; (c) $\cos\theta_{\rm f\bar f}> -0.50$ and $p_{\rm T} > 50$ GeV, for $\sqrt{s} = 205, 210, 215$ GeV. The errors on the cross sections are as given by `VEGAS`.

Figure Captions

[1] Differential distribution in $\cos\theta_{\rm B}$ (see the text for the definition depending on the final state), for processes (1)–(2), in the channels: (a) jjjj, (b) jj$\tau\nu_\tau$, (c) $\tau\nu_\tau\tau\nu_\tau$; for three different values of CM energy, before any cut. Spectra are normalised to one. Continuous line: W^+W^-; dashed line: H^+H^-.

[2] Differential distribution in $\cos\theta_{\rm f\bar f}$ (see the text for the definition depending on the final state), W and H bosons, for processes (1)–(2), in the channels: (a) jjjj, (b) jj$\tau\nu_\tau$, (c) $\tau\nu_\tau\tau\nu_\tau$; for three different values of CM energy, before any cut. Spectra are normalised to one. Continuous line: W^+W^-; dashed line: H^+H^-.

[3] Differential distribution in $p_{\rm T}$ (see the text for the definition depending on the final state), for processes (1)–(2), in the channels: (a) jjjj, (b) jj$\tau\nu_\tau$, (c) $\tau\nu_\tau\tau\nu_\tau$; for three different values of CM energy, before any cut. Spectra are normalised to one. Continuous line: W^+W^-; dashed line: H^+H^-.

[4] Differential distribution in $M_{\rm f\bar f}$ (see the text for the definition depending on the final state), for processes (1)–(2), in the channels: (a) jjjj, (b) jj$\tau\nu_\tau$, (c) $\tau\nu_\tau\tau\nu_\tau$; for three different values of CM energy, after the following cuts: (a) and (b) $|\cos\theta_{\rm B}| < 0.60$ (for all $\sqrt{s}$), plus $\cos\theta_{\rm f\bar f}< -0.88(-0.80)[-0.72]$ and $p_{\rm T} < 24(34)[40]$ GeV, in correspondence of $\sqrt{s} = 205(210)[215]$ GeV; (c) $\cos\theta_{\rm f\bar f}> -0.50$ and $p_{\rm T} > 50$ GeV, for $\sqrt{s} = 205, 210, 215$ GeV. Spectra are normalised to the total cross sections. Continuous line: W^+W^-; dashed line: H^+H^-.

σ (fb)		
$\sqrt{s}$ (GeV)	$W^+W^- \to$ jjjj	$H^+H^- \to$ jjjj
205	$6904. \pm 10.$	$(1212.11 \pm 0.31) \times 10^{-4}$
210	$6850. \pm 11.$	$(2967.12 \pm 0.77) \times 10^{-4}$
215	$6777. \pm 11.$	$(4852.04 \pm 1.30) \times 10^{-4}$
no kinematic cuts		
205	278.9 ± 1.1	$(9.5164 \pm 0.0034) \times 10^{-2}$
210	458.4 ± 1.8	$(22.9843 \pm 0.0090) \times 10^{-2}$
215	616.1 ± 2.0	$(33.112 \pm 0.010) \times 10^{-2}$
after kinematic cuts		
$M_W \approx 80$ GeV	$\tan\beta = 1.5$	$M_H \approx 100$ GeV

Tab. Ia

σ (fb)		
$\sqrt{s}$ (GeV)	$W^+W^- \to \mathrm{jj}\tau\nu_\tau$	$H^+H^- \to \mathrm{jj}\tau\nu_\tau$
205	2300.79 ± 3.34	1.6207 ± 0.0042
210	2282.68 ± 3.58	3.967 ± 0.010
215	2258.24 ± 3.82	6.488 ± 0.017
no kinematic cuts		
205	2.140 ± 0.014	1.2835 ± 0.0044
210	4.651 ± 0.024	3.1427 ± 0.0051
215	6.714 ± 0.031	5.1384 ± 0.0085
after kinematic cuts		
$M_W \approx 80$ GeV	$\tan\beta = 1.5$	$M_H \approx 100$ GeV

Tab. Ib

σ (fb)		
$\sqrt{s}$ (GeV)	$W^+W^- \to \tau\nu_\tau\tau\nu_\tau$	$H^+H^- \to \tau\nu_\tau\tau\nu_\tau$
205	191.68 ± 0.28	5.4177 ± 0.0014
210	190.17 ± 0.30	13.2620 ± 0.0034
215	188.14 ± 0.32	21.6870 ± 0.0056
no kinematic cuts		
205	35.481 ± 0.085	2.8796 ± 0.0018
210	33.563 ± 0.084	6.9991 ± 0.0044
215	31.555 ± 0.082	11.3539 ± 0.0073
after kinematic cuts		
$M_W \approx 80$ GeV	$\tan\beta = 1.5$	$M_H \approx 100$ GeV

Tab. Ic

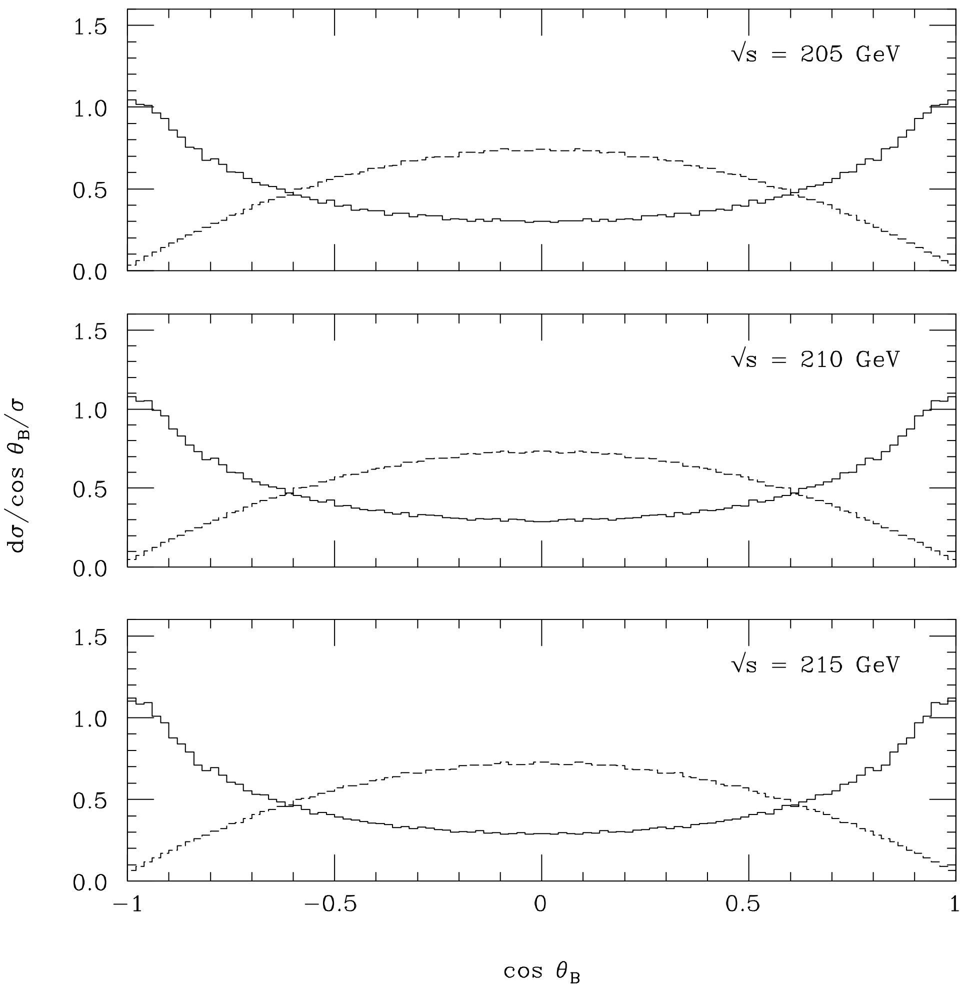

Fig. 1a

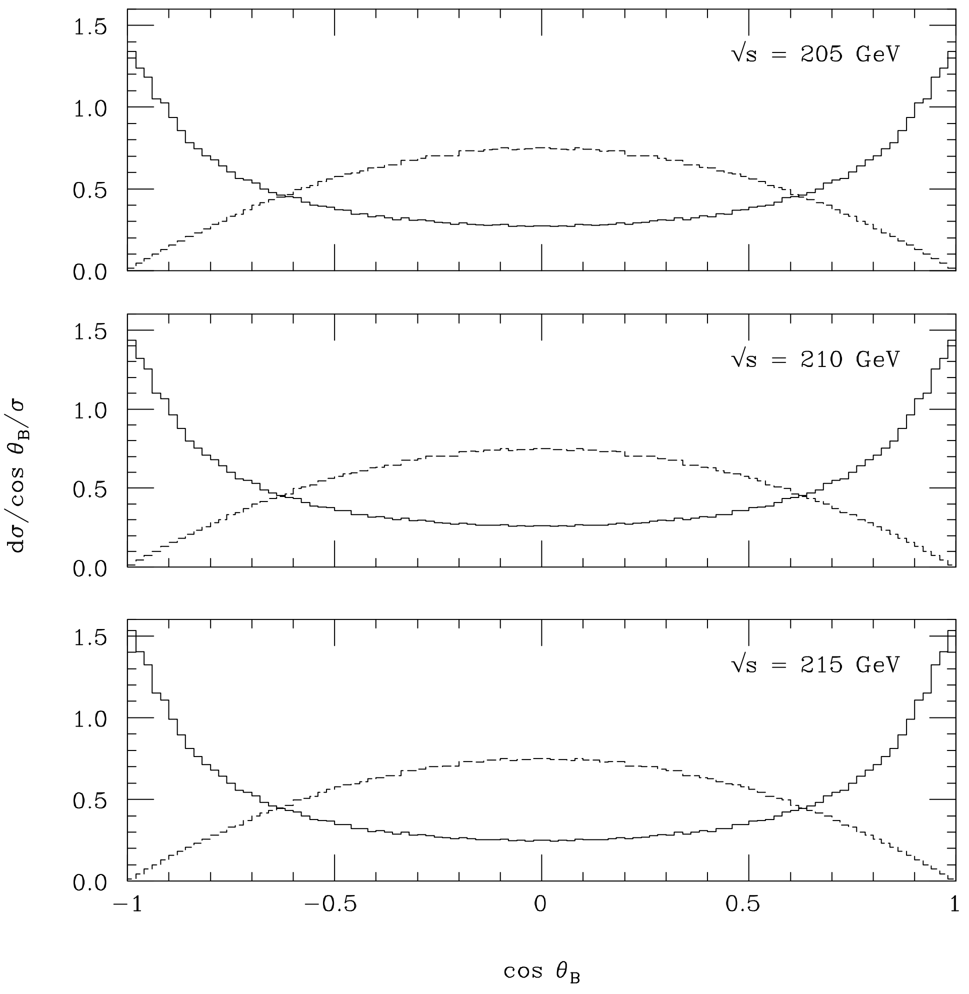

1.5
1.0
0.5
0.0
$\sqrt{s}$ = 205 GeV
$\sqrt{s}$ = 210 GeV
$\sqrt{s}$ = 215 GeV
$d\sigma/\cos\theta_B/\sigma$
−1
−0.5
0
0.5
1
$\cos\theta_B$

Fig. 1b

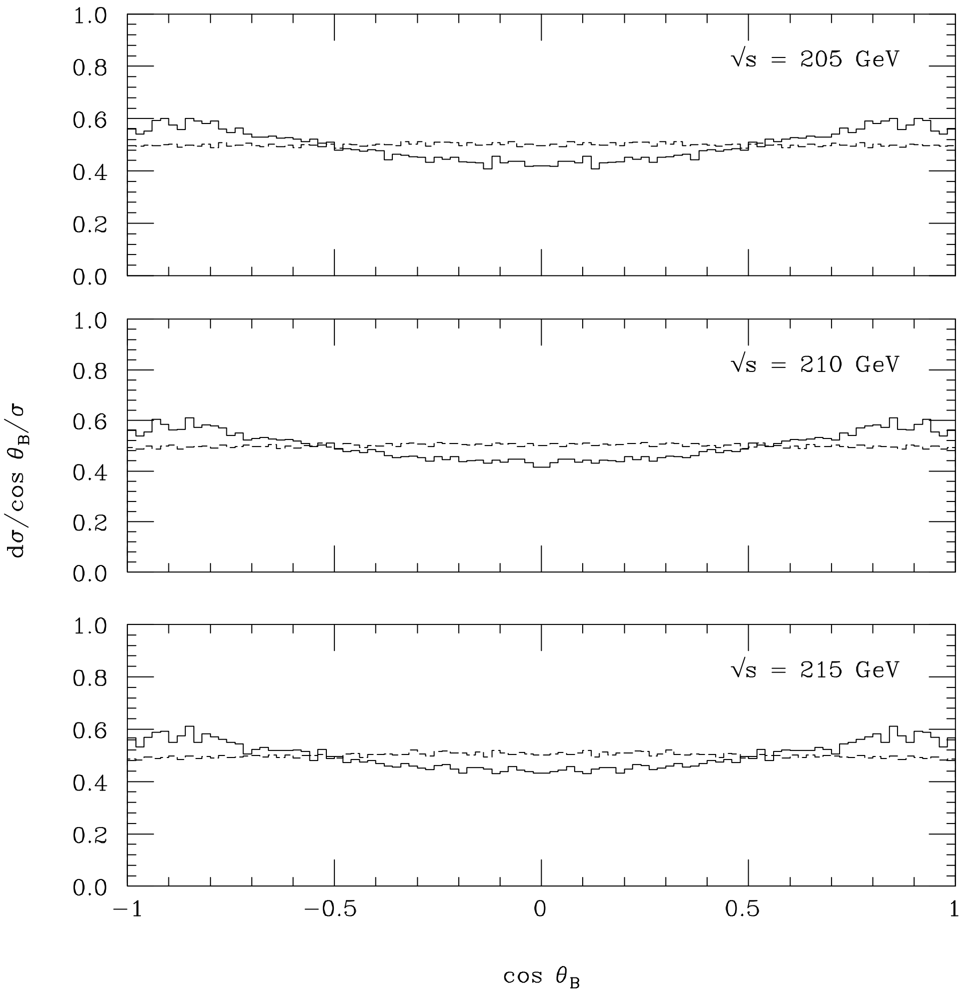

1.0
0.8
0.6
0.4
0.2
0.0
√s = 205 GeV
√s = 210 GeV
√s = 215 GeV
dσ/cos θ_B/σ
−1
−0.5
0
0.5
1
cos θ_B

Fig. 1c

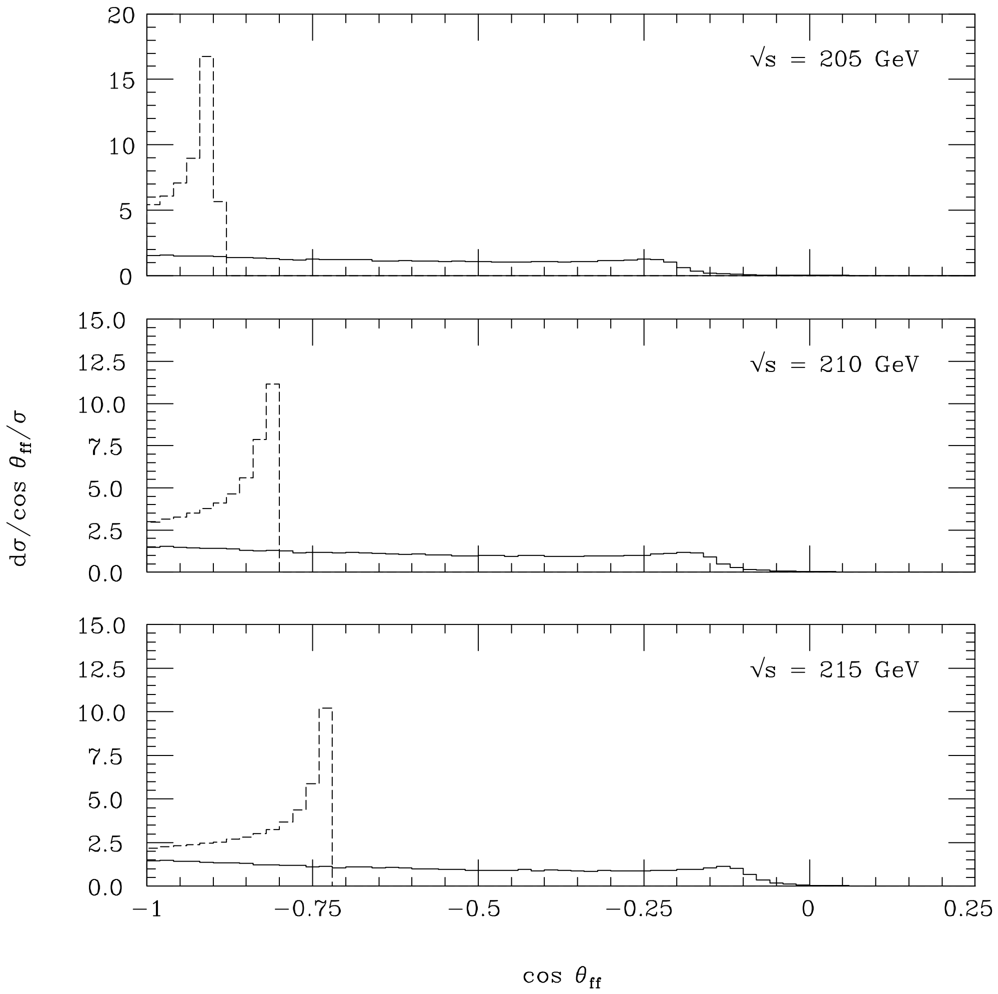
20
15
10
5
0
√s = 205 GeV
15.0
12.5
10.0
7.5
5.0
2.5
0.0
√s = 210 GeV
15.0
12.5
10.0
7.5
5.0
2.5
0.0
√s = 215 GeV
−1
−0.75
−0.5
−0.25
0
0.25
dσ/cos θff/σ
cos θff

Fig. 2a

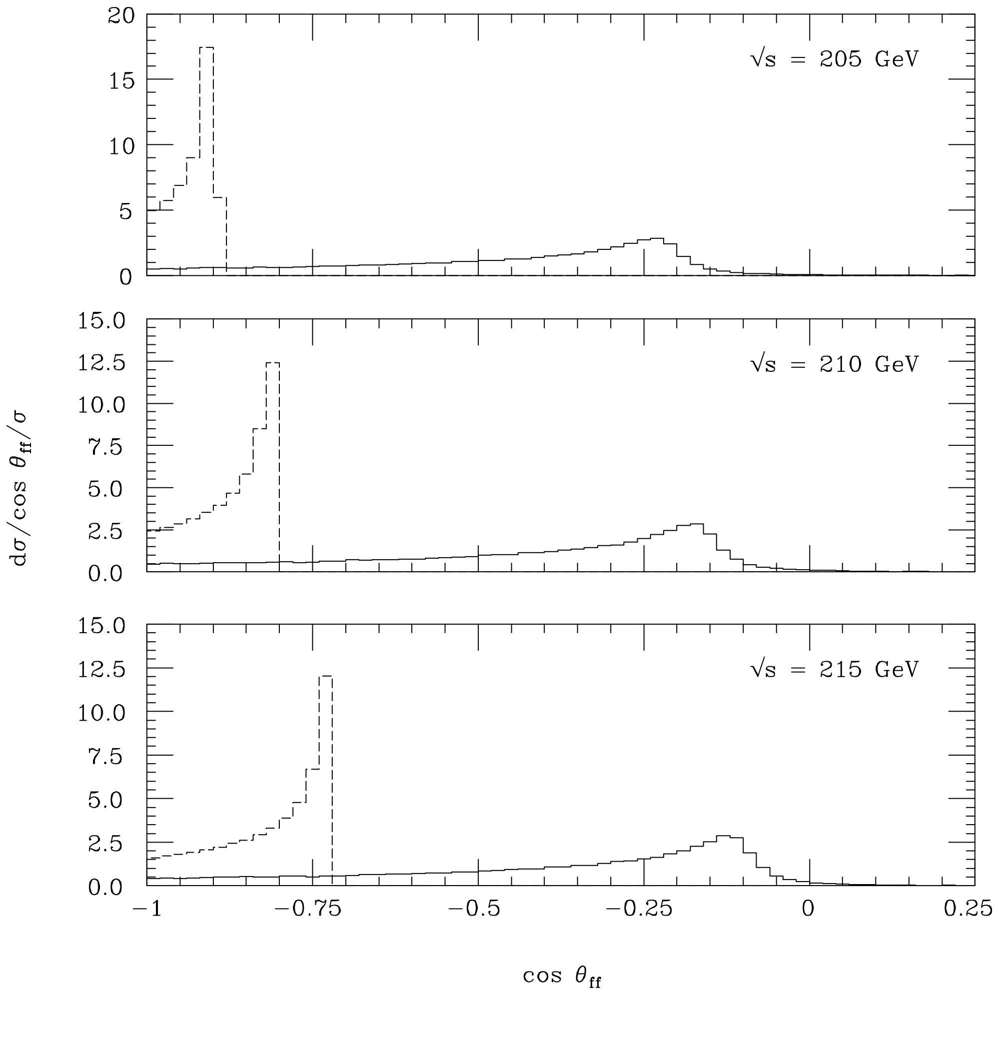

√s = 205 GeV
√s = 210 GeV
√s = 215 GeV
dσ/cos θ_ff/σ
cos θ_ff
20
15
10
5
0
15.0
12.5
10.0
7.5
5.0
2.5
0.0
−1
−0.75
−0.5
−0.25
0
0.25

Fig. 2b

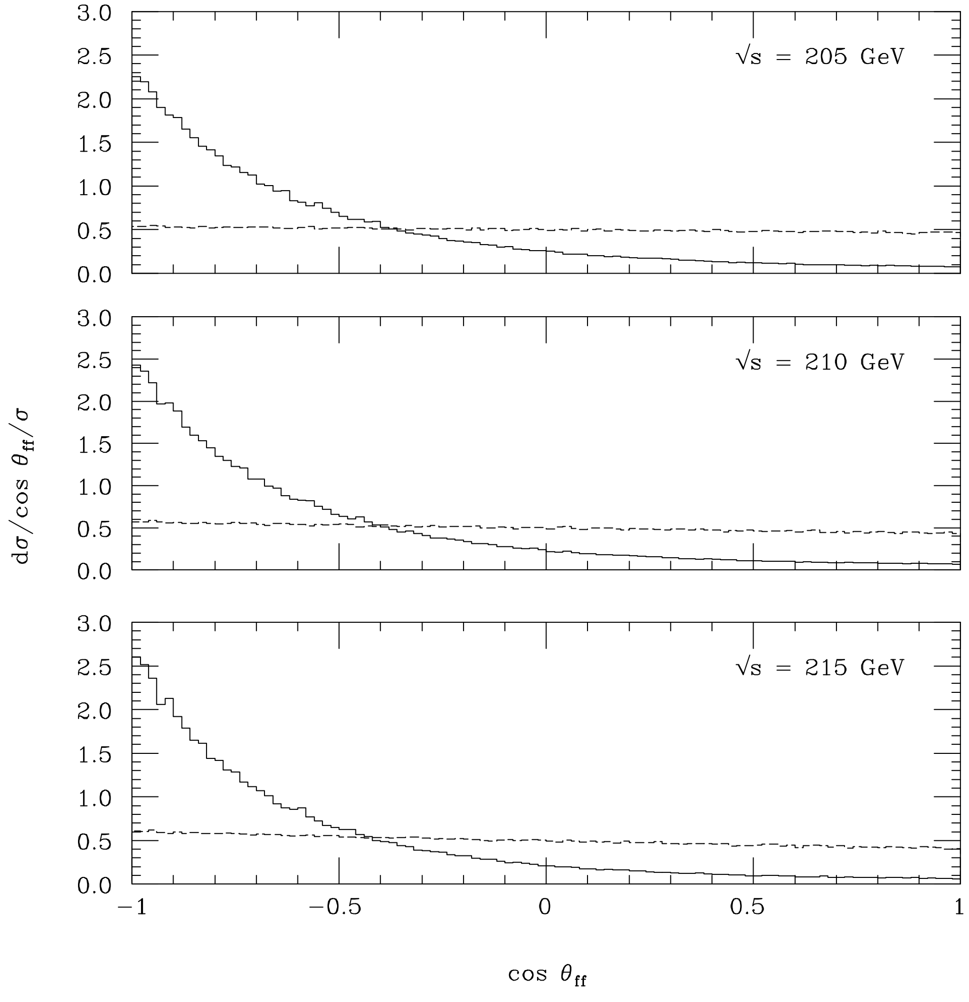

√s = 205 GeV
√s = 210 GeV
√s = 215 GeV
dσ/cos θ_ff/σ
cos θ_ff
3.0
2.5
2.0
1.5
1.0
0.5
0.0
−1
−0.5
0
0.5
1

Fig. 2c

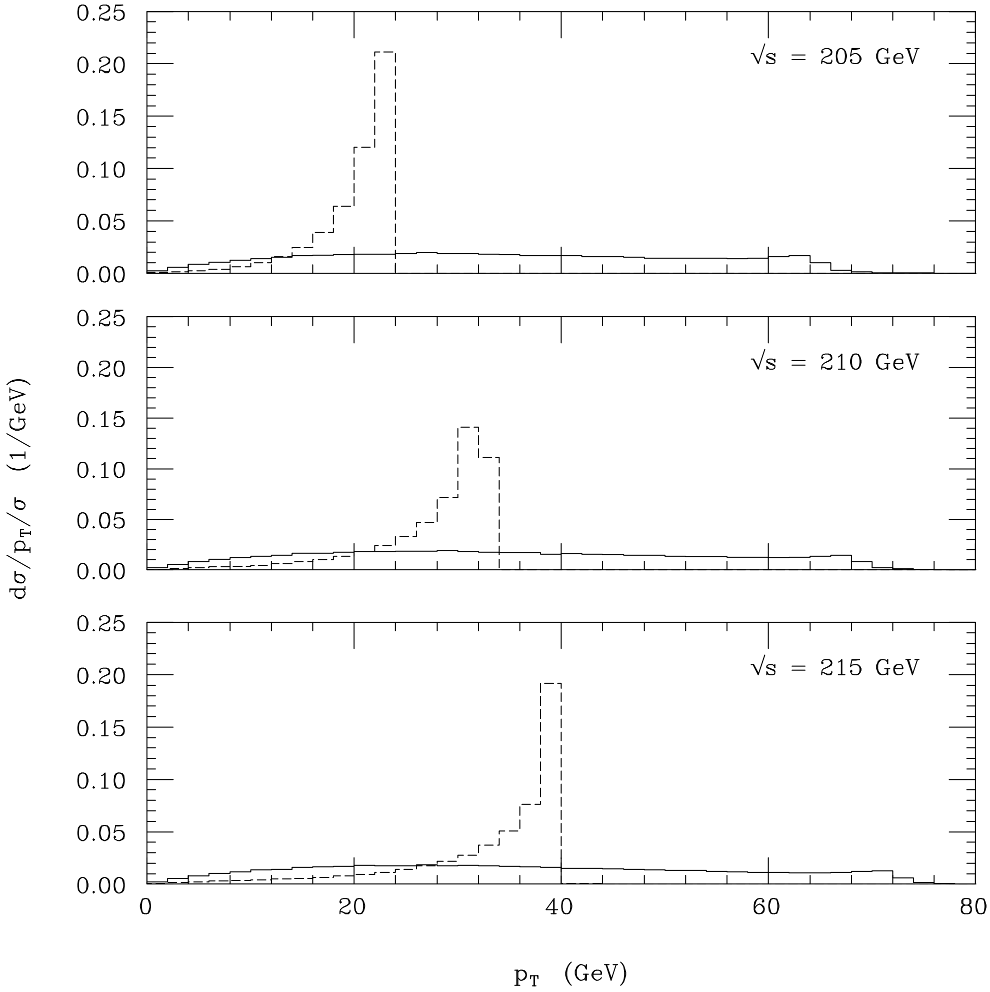

0.25
0.20
0.15
0.10
0.05
0.00
√s = 205 GeV
√s = 210 GeV
√s = 215 GeV
dσ/p_T/σ (1/GeV)
0
20
40
60
80
p_T (GeV)

Fig. 3a

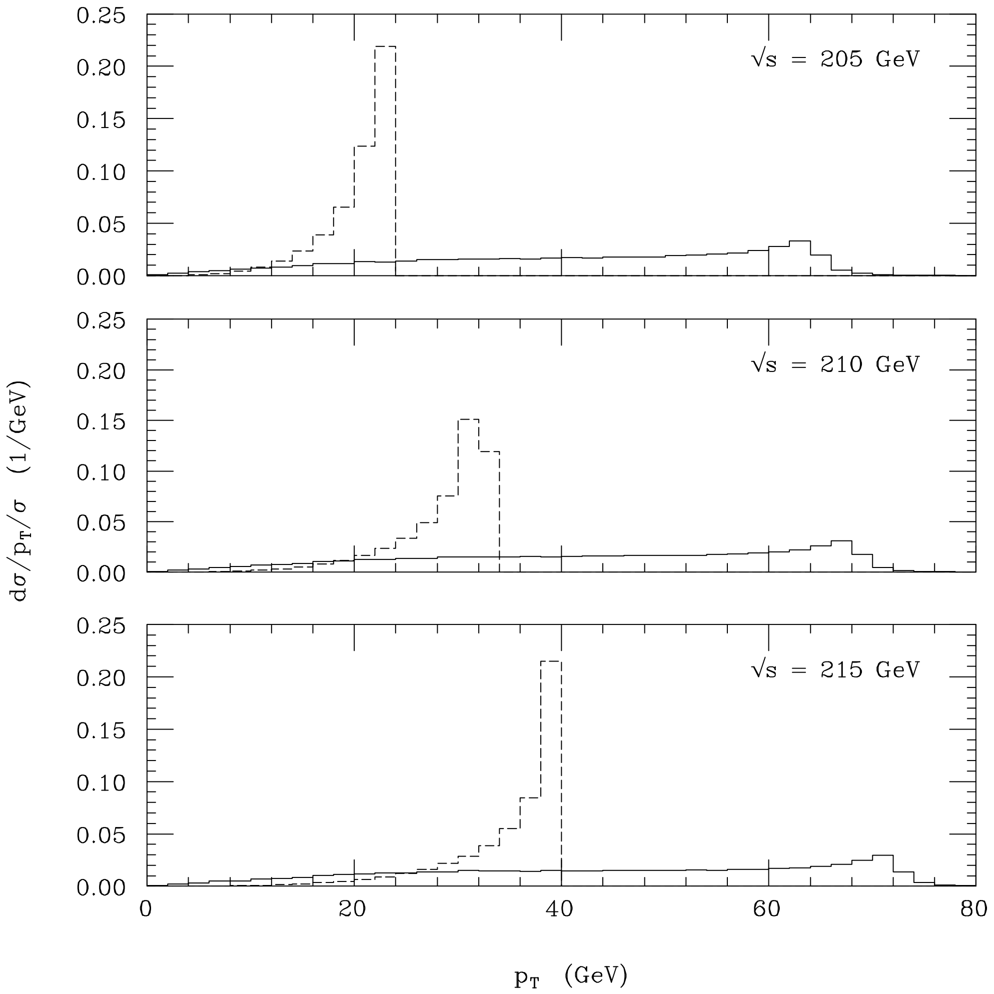
√s = 205 GeV
√s = 210 GeV
√s = 215 GeV
dσ/p_T/σ (1/GeV)
p_T (GeV)
0.25
0.20
0.15
0.10
0.05
0.00
0
20
40
60
80

Fig. 3b

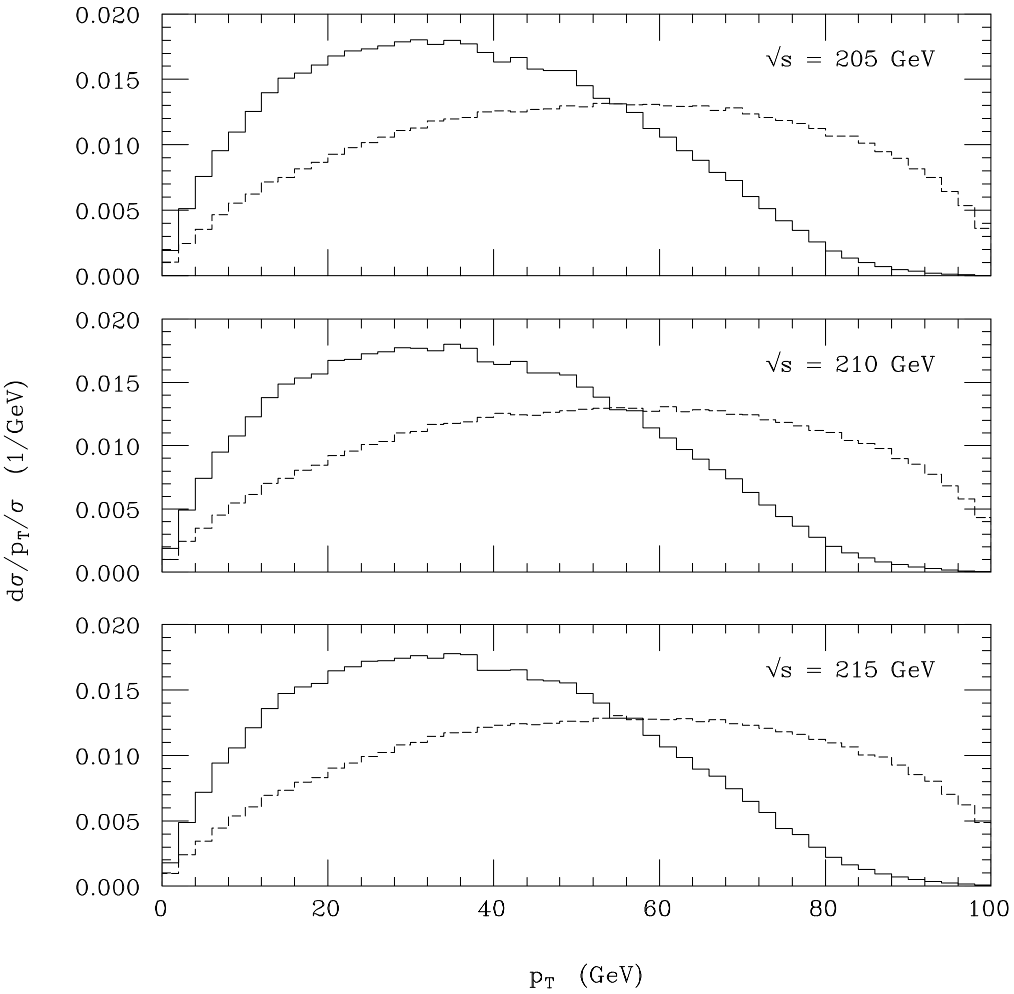

√s = 205 GeV
√s = 210 GeV
√s = 215 GeV
0.020
0.015
0.010
0.005
0.000
0
20
40
60
80
100
dσ/p_T/σ (1/GeV)
p_T (GeV)

Fig. 3c

After kinematic cuts

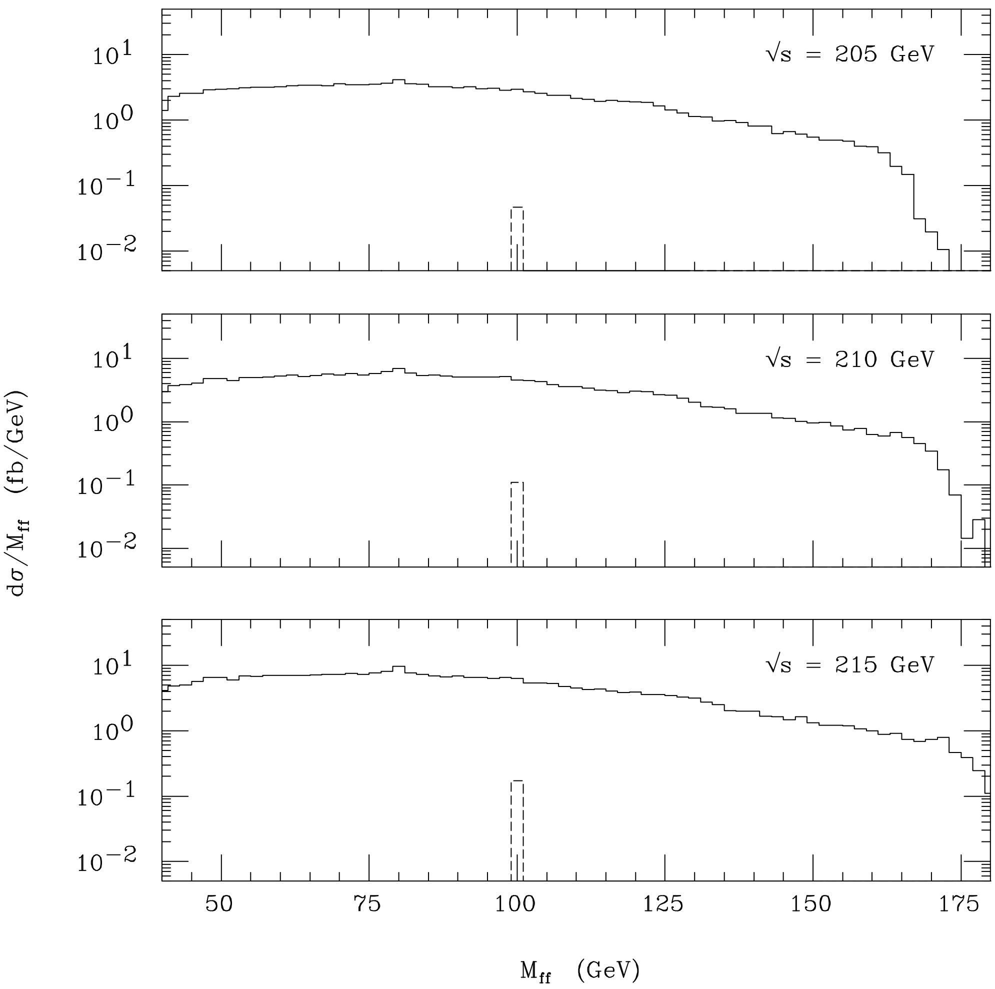

Fig. 4a

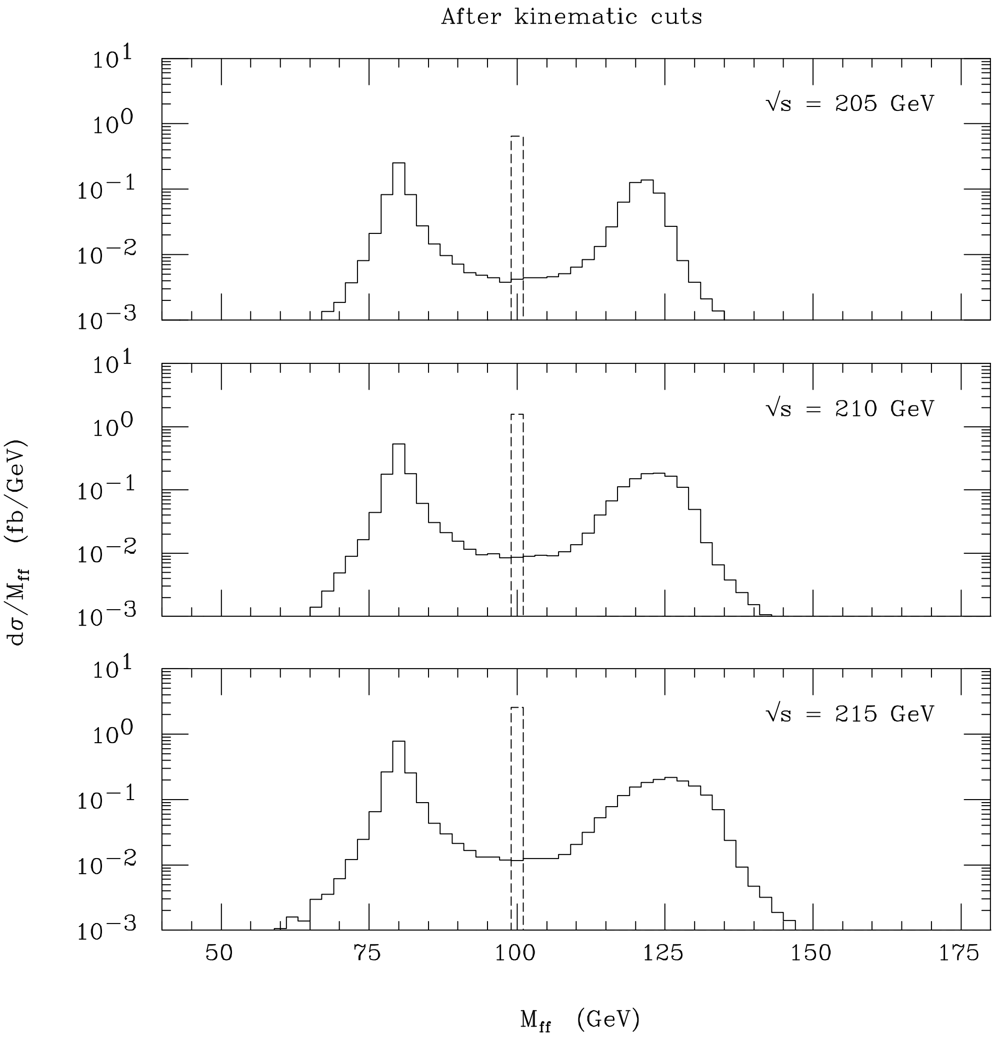
After kinematic cuts
$\sqrt{s}$ = 205 GeV
$\sqrt{s}$ = 210 GeV
$\sqrt{s}$ = 215 GeV
$d\sigma/M_{ff}$ (fb/GeV)
10^{1}
10^{0}
10^{-1}
10^{-2}
10^{-3}
50
75
100
125
150
175
M_{ff} (GeV)

Fig. 4b

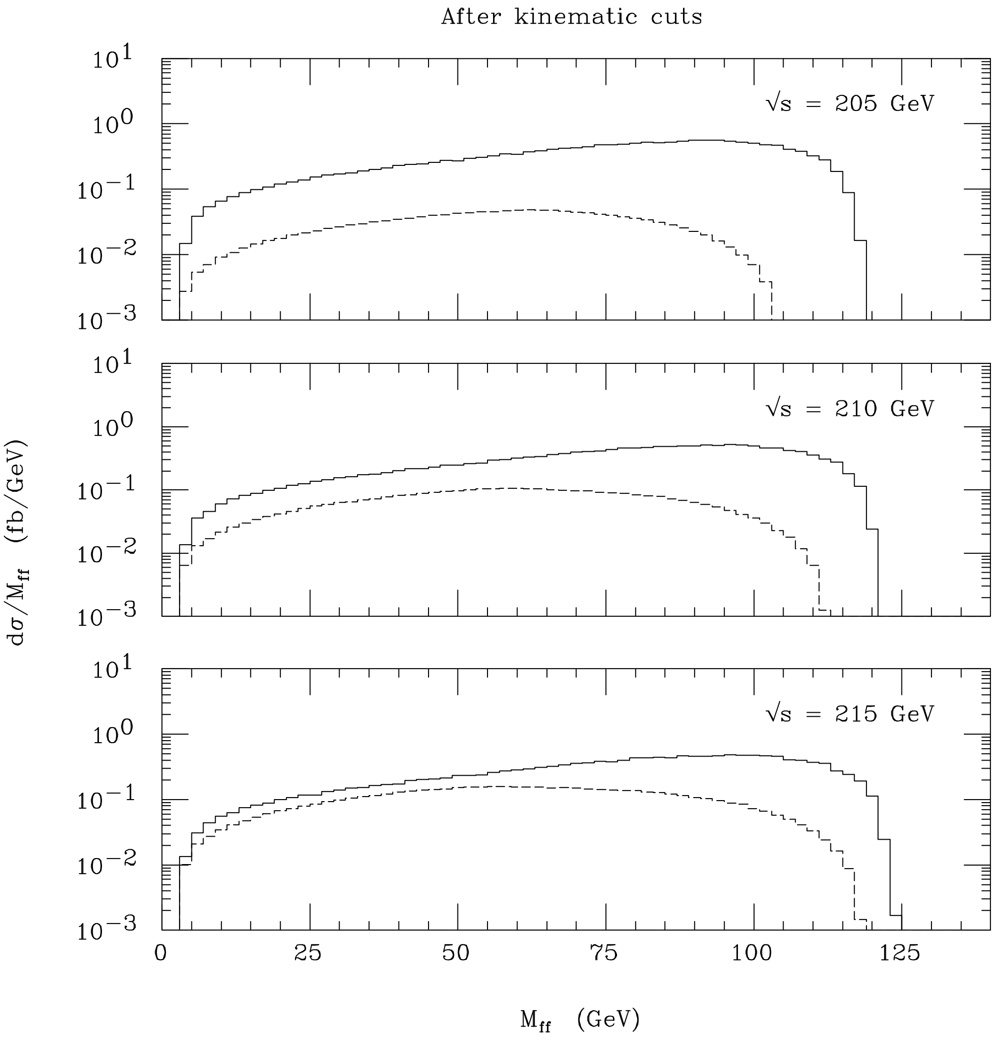

After kinematic cuts
√s = 205 GeV
√s = 210 GeV
√s = 215 GeV
10^{1}
10^{0}
10^{-1}
10^{-2}
10^{-3}
$d\sigma/M_{ff}$ (fb/GeV)
0
25
50
75
100
125
M_{ff} (GeV)

Fig. 4c